

1N-34  
214 614

# NASA

## MEMORANDUM

EFFECTS OF YAW ON THE HEAT TRANSFER TO A  
BLUNT CONE-CYLINDER CONFIGURATION  
AT A MACH NUMBER OF 1.98

By Roland D. English

Langley Research Center  
Langley Field, Va.

**NATIONAL AERONAUTICS AND  
SPACE ADMINISTRATION**

**WASHINGTON**

November 1958

Declassified April 12, 1961



## NATIONAL AERONAUTICS AND SPACE ADMINISTRATION

NASA MEMO 10-8-58L

EFFECTS OF YAW ON THE HEAT TRANSFER TO A  
BLUNT CONE-CYLINDER CONFIGURATION

AT A MACH NUMBER OF 1.98\*

By Roland D. English

## SUMMARY

A heat-transfer investigation has been made on a blunt cone-cylinder model at a Mach number of 1.98 at yaw angles from  $0^\circ$  to  $9^\circ$ . The results indicate that, except for the hemispherical nose, the heat-transfer coefficient increased on the windward side and decreased on the leeward side as yaw angle was increased. In general, the increase in heat transfer on the windward side was higher than the corresponding decrease on the leeward side. A comparison with theory (NACA Technical Note 4208) yielded agreement which was, in general, within 10 percent on the cone at all test conditions and on the cylinder at an angle of yaw of  $0^\circ$ .

## INTRODUCTION

A general investigation to determine the convective heat transfer to various wings, bodies, and combinations and to assess the applicability of existing theories to the prediction of heat transfer is being carried out at the Langley Pilotless Aircraft Research Division. Practically all of the past investigations have been made with the model axis parallel to the direction of flow. The necessity for maneuvering flight for interceptor- and tracking-type missiles requires that they travel at appreciable angles of yaw. The need exists, then, for data concerning the effects of yaw on the aerodynamic heat transfer to missile components. In an effort to partially fill the need, an investigation has been made at a Mach number of 1.98 of the convective heat transfer to a blunt  $20^\circ$  total-angle-cone-cylinder configuration at angles of yaw from  $0^\circ$  to  $9^\circ$ . The tests were made in the preflight jet of the Langley Pilotless Aircraft Research Station at Wallops Island, Va.

---

\*Title, Unclassified.

## SYMBOLS

$c_p$	specific heat of air at constant pressure, Btu/lb-°F
$h$	aerodynamic convective heat-transfer coefficient, Btu/(sq ft)(sec)(°F)
$k$	thermal conductivity of air, (Btu)(ft)/(sq ft)(sec)(°F)
$N_{Pr}$	Prandtl number, $c_p\mu/k$
$p_l$	local static pressure, lb/sq ft
$p_t$	model stagnation pressure, lb/sq ft
$q$	specific heat of Inconel, Btu/(lb)(°F)
$t$	model skin thickness, ft
$T_w$	skin temperature, °R
$T_l$	local static temperature, °R
$T_{aw}$	adiabatic wall temperature, °R
$T_t$	stagnation temperature, °R
$x$	distance along the model measured from the stagnation point, in. or ft
$\mu$	coefficient of viscosity, lb/ft-sec
$\rho_w$	weight density of Inconel, lb/cu ft
$\tau$	time, sec
$\psi$	angle of yaw, deg

## MODEL AND TESTS

The model used in these tests consisted of a 20°-total-angle cone with a 1/2-inch-radius hemispherical nose and a 7-inch-diameter

cylindrical afterbody. The model was spun from 1/32-inch (nominal thickness) Inconel and was supported by a wood former which was turned to the internal dimensions of the skin and slotted to provide clearance for the thermocouple leads and pressure tubes. Fourteen iron-constantan thermocouples were located along an element of the model and 13 pressure orifices were located along the element 180° circumferentially from the thermocouples. The dimensions of the model and locations of the thermocouples and pressure orifices are given in the sketch of figure 1. Measured skin thicknesses at the locations of the thermocouples is given in table I.

The tests were made in the preflight jet of the Langley Pilotless Aircraft Research Station at Wallops Island, Va., with the 27- by 27-inch nozzle being used. All tests were made at sea-level atmospheric conditions at a Mach number of 1.98 and a Reynolds number, based on a length of one foot, of about  $12 \times 10^6$ . Stagnation temperature was practically constant during each test but varied from test to test from 1,020° R to 1,080° R. Tests were made at yaw angles of 0°, ±3°, ±6°, and ±9°. During the tests the thermocouples and pressure orifices were located in the plane of yaw. Skin temperatures were measured by iron-constantan thermocouples and local pressures were measured by Statham strain-gage type pressure cells. Both pressures and temperatures were recorded on Consolidated oscillograph recorders. A photograph of the model mounted in the test section is shown in figure 2. A detailed description of the preflight jet is given in reference 1.

#### DATA REDUCTION

If terms for radiation and heat conduction along the model skin, which were negligible, are omitted, the equation for convective heat-transfer coefficient is

$$h = \frac{\rho_w q t \frac{dT_w}{d\tau}}{T_{aw} - T_w}$$

The physical properties of Inconel which were used are 518 lb/cu ft for the weight density and values of specific heat from the curve in figure 3. The values of  $dT_w/d\tau$  were obtained by graphically differentiating plots of the skin temperature measured during the tests. (A sample plot is given in fig. 4.) Adiabatic wall temperature was calculated from

$$T_{aw} = N_{Pr}^{1/3} (T_t - T_l) + T_l$$

where  $N_{Pr}^{1/3}$ , the theoretical recovery factor for a turbulent boundary layer, was evaluated from the physical properties of air at local static temperature. The results of the tests indicated that the boundary layer was turbulent at thermocouples 2 to 14 for all angles of yaw and the data were reduced accordingly. Values of  $T_1$  were calculated from the pressure distributions and stagnation temperatures measured during the tests. Pressure distributions are presented in figure 5 and table II. The coordinate  $x$  in figure 5 is measured from the stagnation point.

#### EXPERIMENTAL ACCURACY

The data scatter resulting from known accuracy limitations of the instrumentation and estimated record-reading errors for the heat-transfer coefficients presented herein was within  $\pm 10$  percent.

#### RESULTS AND DISCUSSION

The basic heat-transfer data obtained in this investigation are presented in figure 6 where the variation along an element of the model is shown for all yaw angles. Test points are missing for some yaw angles at thermocouple 7 because of failure of this thermocouple to record during some runs. The reader will undoubtedly note the sudden variation in heat-transfer coefficient in figure 6 from thermocouple 6 to thermocouple 8. There is no known reason for this variation. It may be noted that it occurs for all angles of yaw on both the windward and leeward sides of the model.

The effect of yaw on heat-transfer coefficient is shown in figure 7 where the data of figure 6 are cross-plotted as a function of yaw angle. The variation in heat-transfer coefficient on the hemispherical nose (thermocouples 1 and 2) shown in figure 7 is random and is probably the result of experimental errors. On the rest of the model, except for isolated discrepancies which may be attributed to experimental error, the heat-transfer coefficient increases on the windward side and decreases on the leeward side as yaw angle is increased. The largest variation in heat-transfer coefficient in figure 7 occurs at the junction of the hemisphere and the cone (thermocouple 3) where the variation in local flow conditions is the largest. It is impossible to determine accurately the rate of change of heat-transfer coefficient with angle of yaw due to data scatter. It is evident, however, that the increase in heat-transfer coefficient on the windward side is larger than the decrease on the leeward side.

The data obtained in these tests are compared with theory in figure 8. The theory of Sibulkin (ref. 2) modified for compressibility effects was used for theoretical heat transfer at the stagnation point. The theory of Van Driest as presented in reference 3 was modified according to reference 4 and used for the conical part of the model at an angle of yaw of  $0^\circ$ . Theoretical heat transfer of the yawed cone was calculated using the method of reference 5 in combination with the calculations for the unyawed cone. The flat-plate theory of Van Driest unmodified, is compared with the experimental data on the cylindrical afterbody. At the stagnation point (thermocouple 1), theory is considerably higher than the experimental data for all test conditions. It should be noted here that the experimental data showed a decrease in heat transfer during each run at thermocouple 1. The decrease was well over the limits of experimental accuracy indicating that the skin in the vicinity of this thermocouple was losing heat to the wood support. Consequently, the measured heat-transfer coefficients are lower than the true values, thereby partially accounting for the disagreement with theory. On the conical part of the model, theory is generally within 10 percent of the experimental data at all yaw angles. On the cylindrical part of the model, theory is in good agreement with experiment only at zero angle of yaw. It should be noted that the theories used take no account of the possible effects of the small temperature gradients which existed on the model skin during the tests.

#### CONCLUDING REMARKS

Tests at a Mach number of 1.98 on a  $20^\circ$  total-angle cone with a hemispherical nose and a cylindrical afterbody indicate that, except for the nose, heat transfer increased on the windward side and decreased on the leeward side as angle of yaw increased. In general, the increase on the windward side was larger than the corresponding decrease on the leeward side. A comparison with theory (NACA Technical Note 4208) yielded agreement which was generally within 10 percent on the cone at all angles of yaw and on the cylinder at an angle of yaw of  $0^\circ$ .

Langley Research Center,  
National Aeronautics and Space Administration,  
Langley Field, Va., May 22, 1958.

## REFERENCES

1. Faget, Maxime A., Watson, Raymond S., and Bartlett, Walter A., Jr.: Free-Jet Tests of a 6.5-Inch-Diameter Ram-Jet Engine at Mach Numbers of 1.81 and 2.00. NACA RM L50L06, 1951.
2. Sibulkin, M.: Heat Transfer Near the Forward Stagnation Point of a Body of Revolution. Jour. Aero. Sci. (Readers' Forum), vol. 19, no. 8, Aug. 1952, pp. 570-571.
3. Lee, Dorothy B., and Faget, Maxime A.: Charts Adapted From Van Driest's Turbulent Flat-Plate Theory for Determining Values of Turbulent Aerodynamic Friction and Heat-Transfer Coefficients. NACA TN 3811, 1956.
4. Van Driest, E. R.: The Problem of Aerodynamic Heating. Aero. Eng. Rev., vol. 15, no. 10, Oct. 1956, pp. 26-41.
5. Braun, Willis H.: Turbulent Boundary Layer on a Yawed Cone in a Supersonic Stream. NACA TN 4208, 1958.



TABLE I.- SKIN THICKNESSES

Thermocouple	Thickness, in.
1	0.030
2	.030
3	.030
4	.030
5	.030
6	.030
7	.030
8	.029
9	.029
10	.029
11	.028
12	.028
13	.027
14	.026

TABLE II.- PRESSURE DISTRIBUTIONS

Thermocouple	Values of $p_1/p_t$ for -						
	$\psi = 0^\circ$	Windward side			Leeward side		
		$\psi = 3^\circ$	$\psi = 6^\circ$	$\psi = 9^\circ$	$\psi = 3^\circ$	$\psi = 6^\circ$	$\psi = 9^\circ$
1	1.000						
2	.655	0.655	0.716	0.744	0.593	0.552	0.510
3	.192	.220	.277	.219	.163	.101	.076
4	.233	.251	.292	.332	.216	.209	.239
5	.229	.223	.260	.302	.212	.207	.235
6	.255	.256	.288	.329	.245	.230	.267
7	.240	.248	.277	.307	.232	.222	.249
8	.230	.252	.281	.300	.230	.210	.235
9	.231	.246	.280	.309	.214	.196	.224
10	.228	.238	.284	.314	.212	.200	.231
11	.201	.227	.265	.292	.213	.197	.223
12	.217	.238	.268	.294	.217	.198	.223
13	.141	.154	.181	.194	.136	.125	.139
14	.128	.145	.170	.188	.128	.120	.141

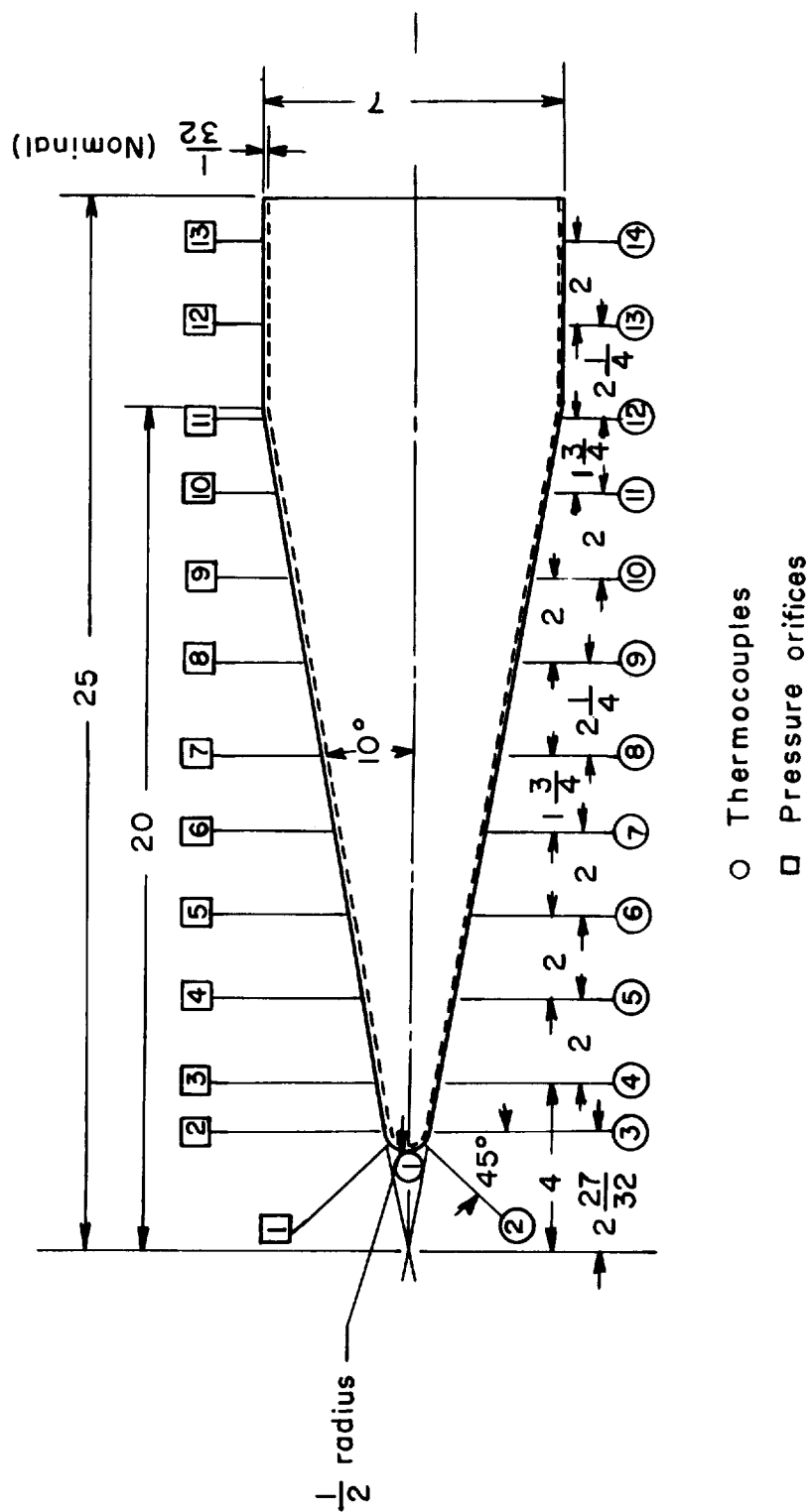
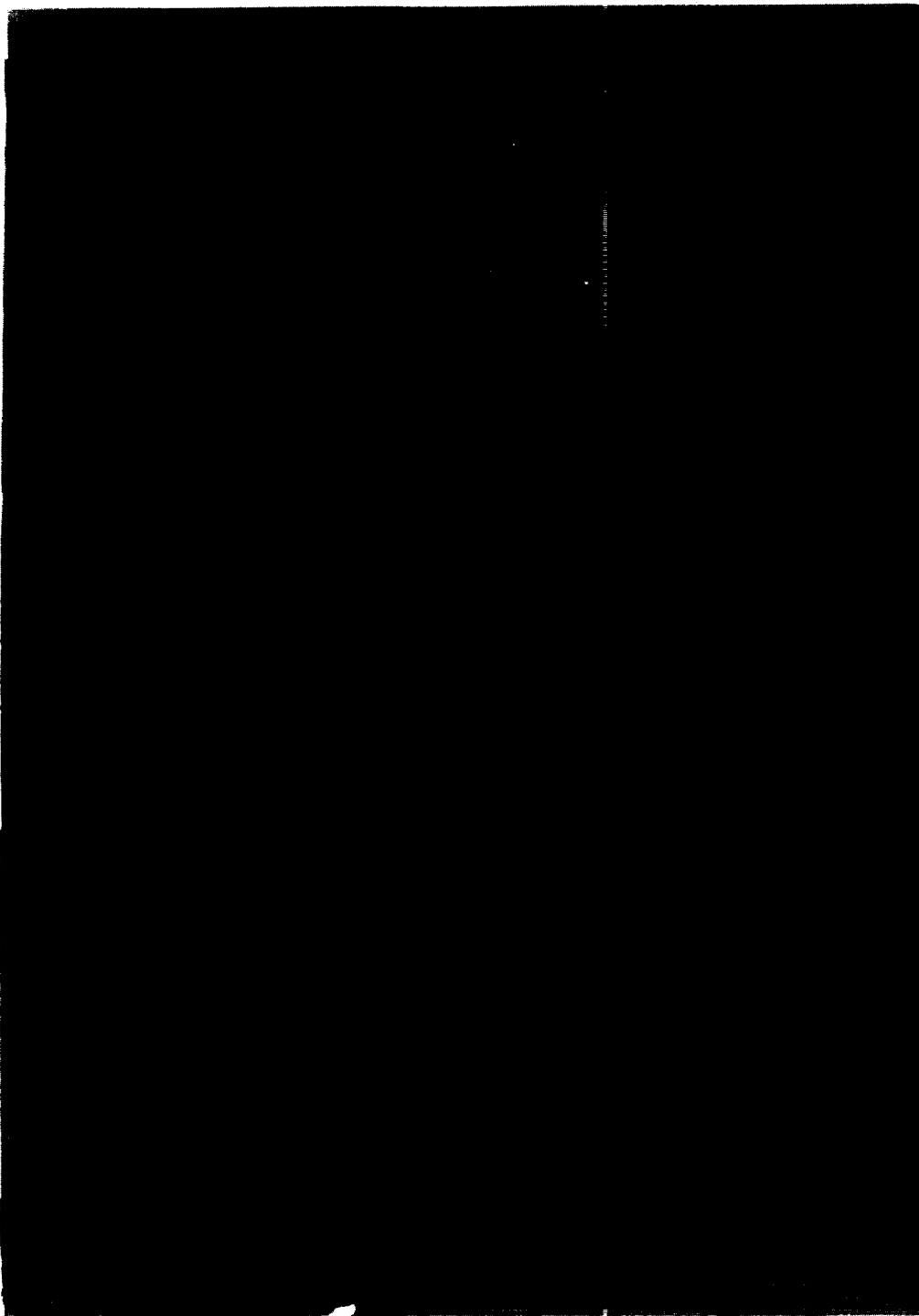


Figure 1.- Sketch of blunt, 20° total-angle-cone—cylinder model. All linear dimensions are in inches.



L-57-1068  
Figure 2.- A photograph of the model mounted in the test section.

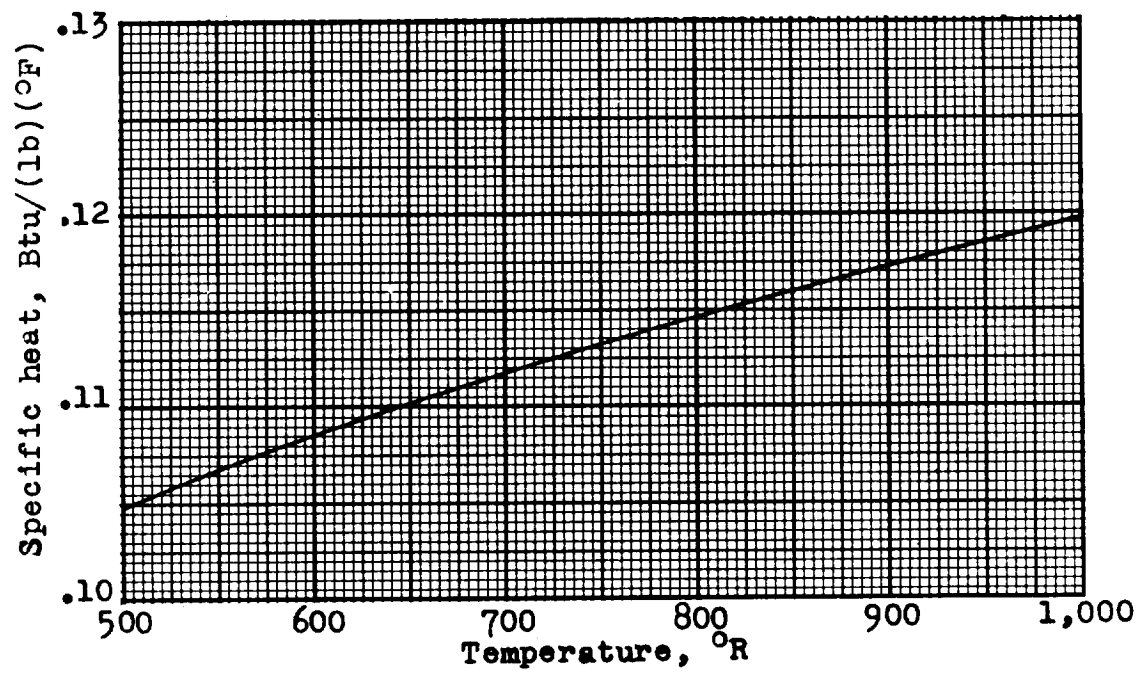


Figure 3.- Variation of specific heat of Inconel with temperature.

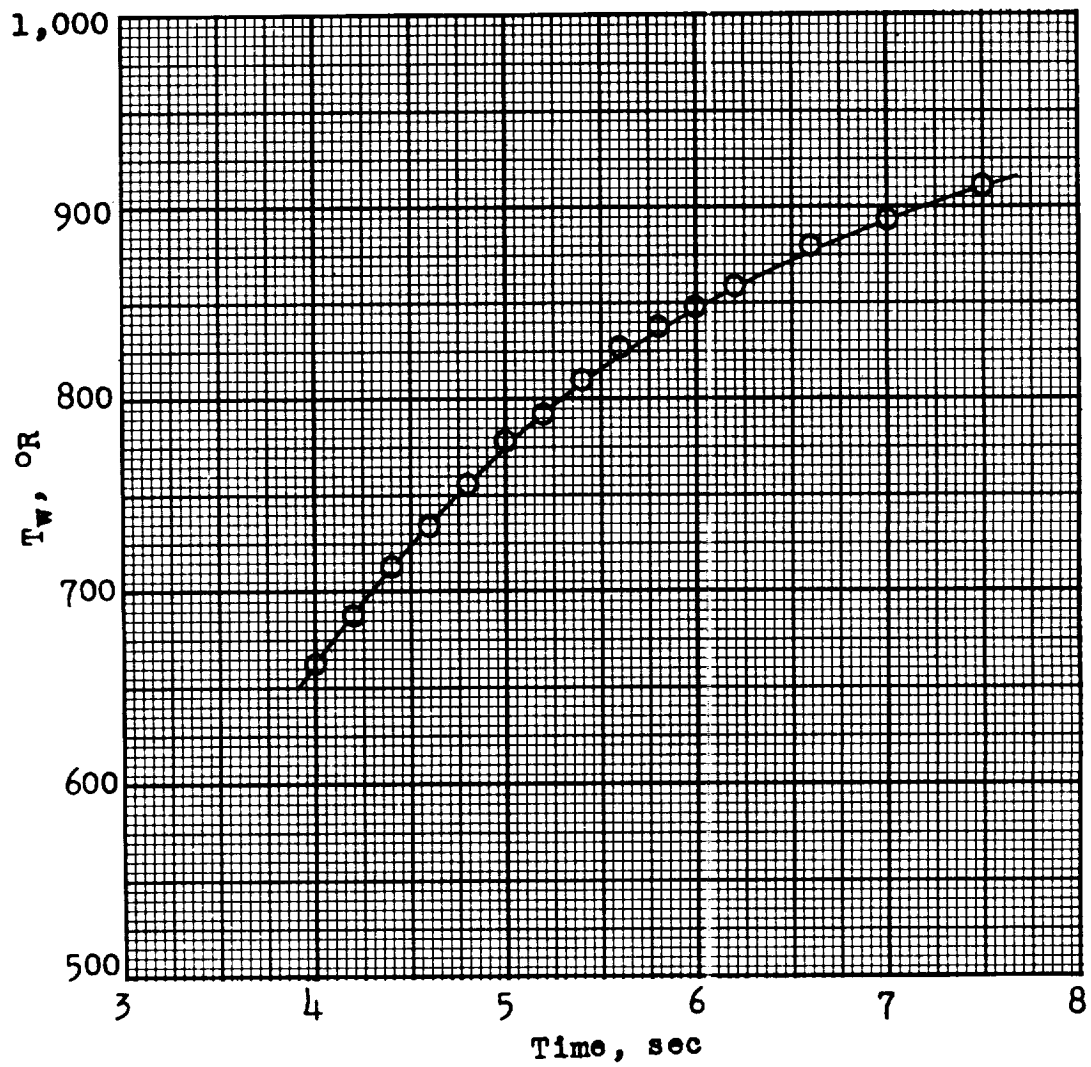
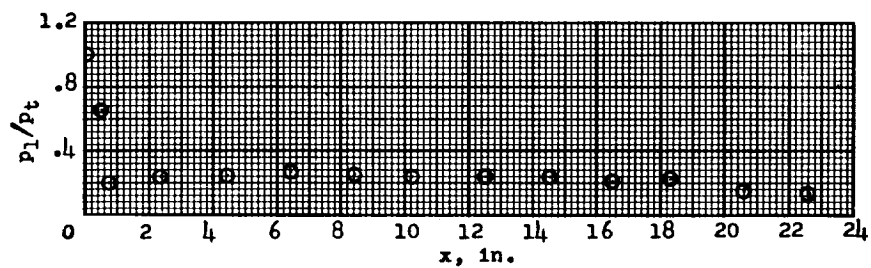
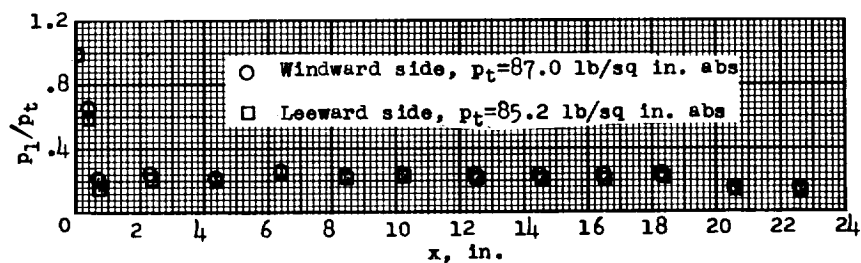


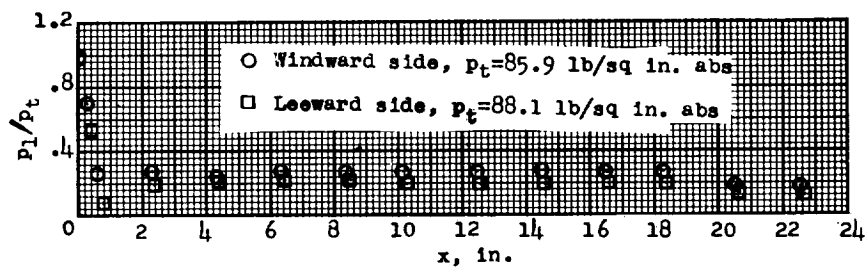
Figure 4.- Typical skin temperature plot. Thermocouple 3;  $\psi = 0^\circ$ .  
Heat-transfer coefficient was calculated at 5 seconds.



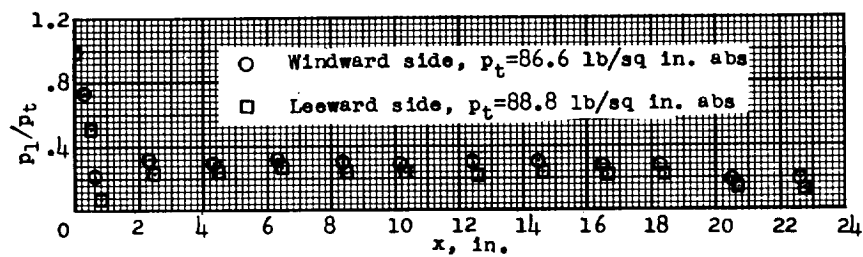
(a)  $\psi = 0^\circ$ ;  $p_t = 85.1$ .



(b)  $\psi = 3^\circ$ .



(c)  $\psi = 6^\circ$ .



(d)  $\psi = 9^\circ$ .

Figure 5.- Pressure distributions.

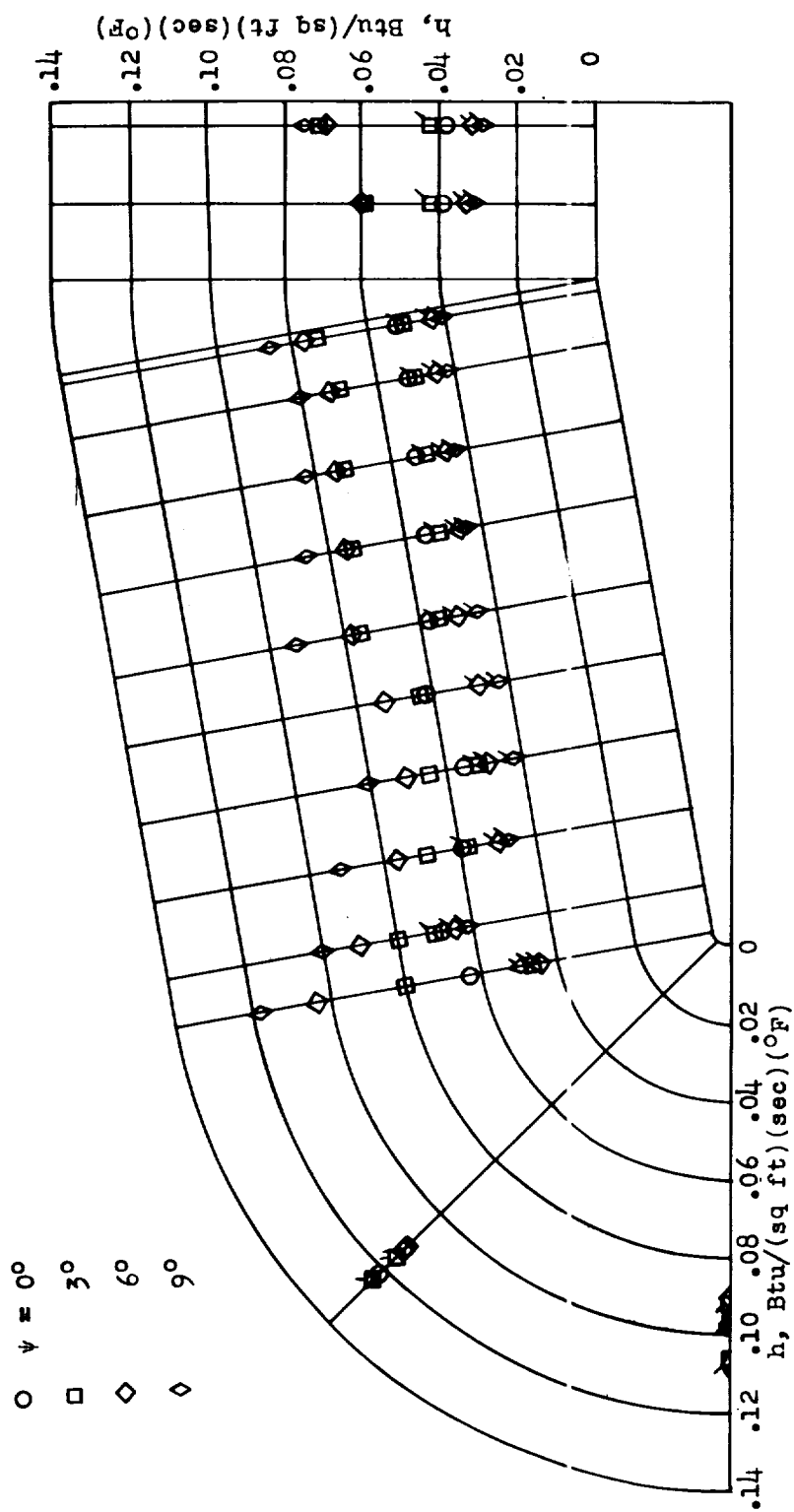


Figure 6.- Variation of heat-transfer coefficient along an element of the model. Flagged symbols denote leeward side.



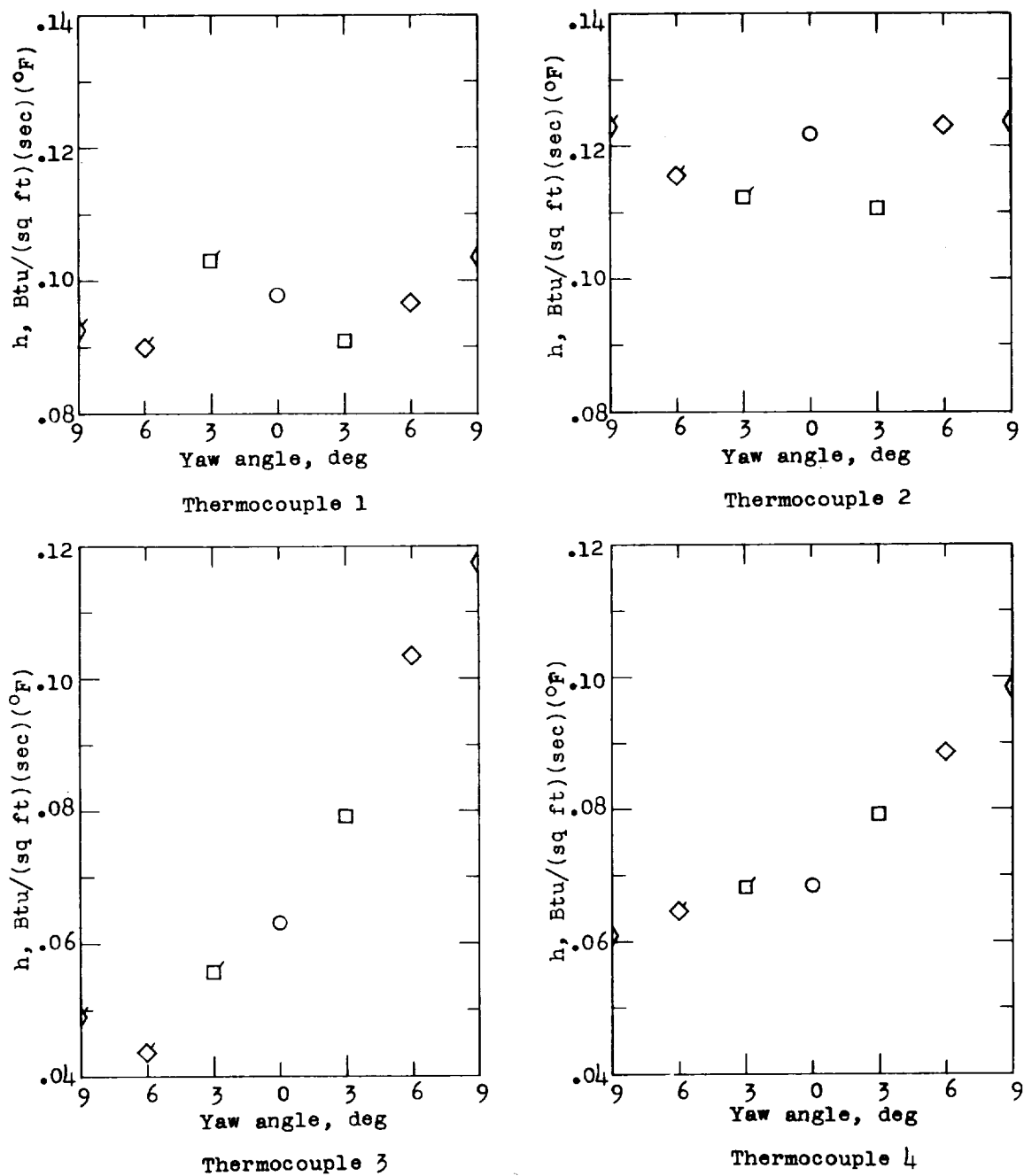


Figure 7.- Variation of heat-transfer coefficient with yaw angle.  
Flagged symbols denote leeward side.

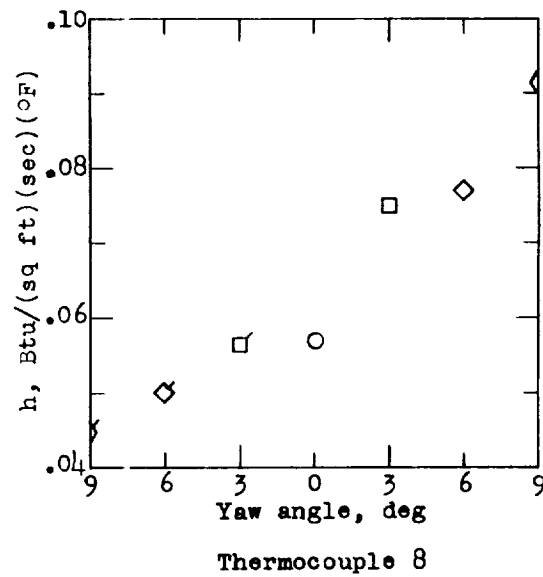
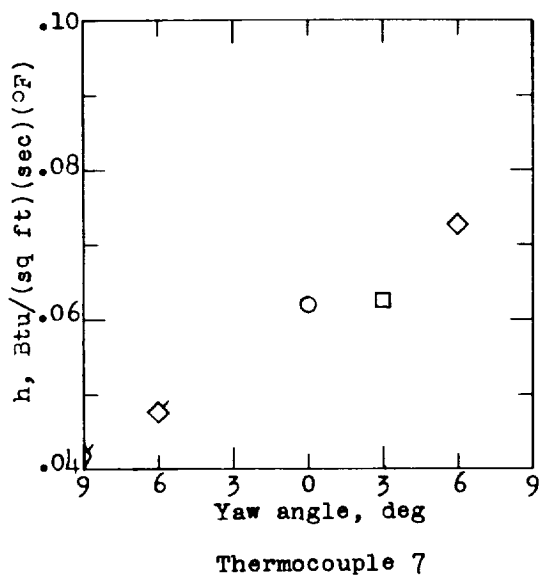
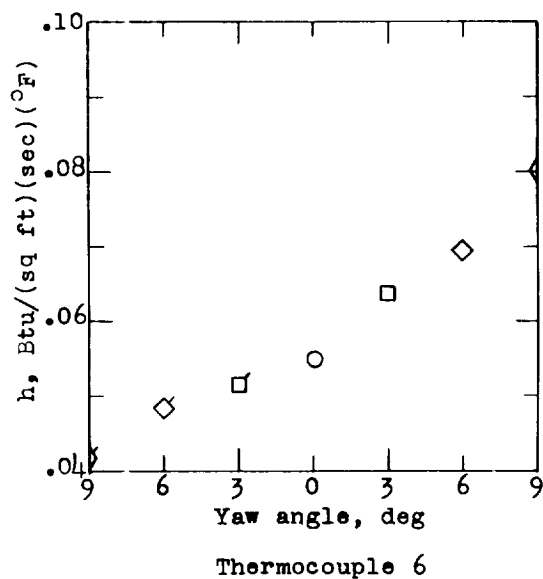
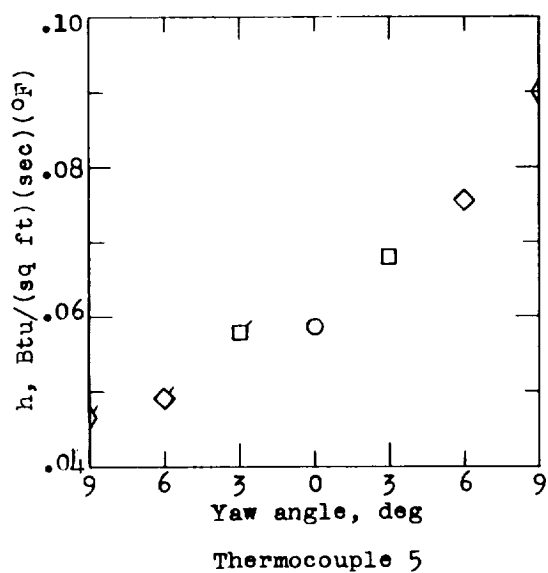


Figure 7.- Continued.

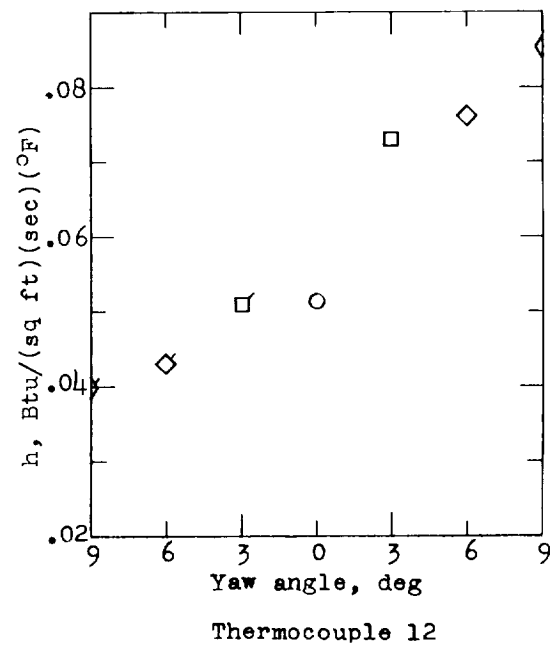
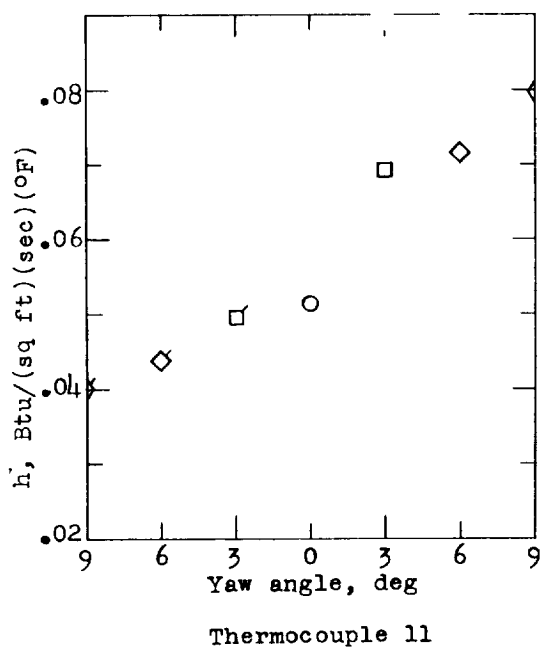
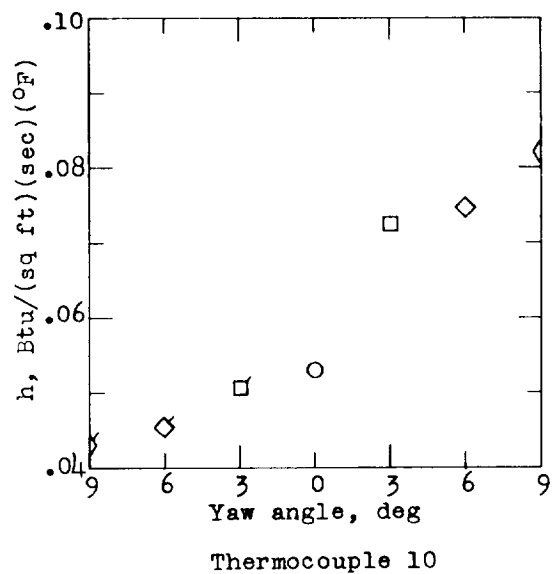
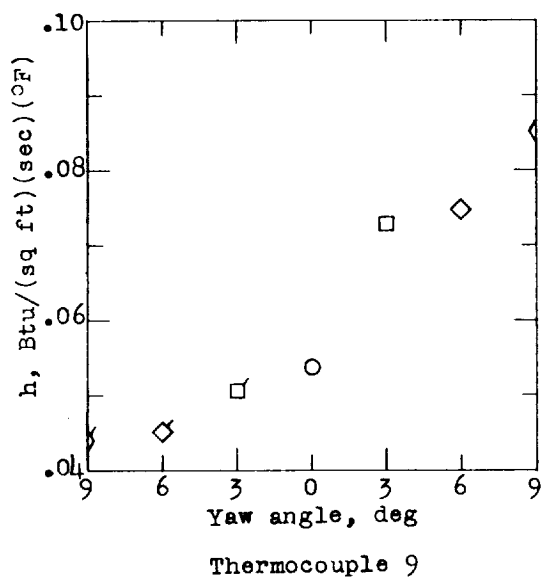


Figure 7.- Continued.

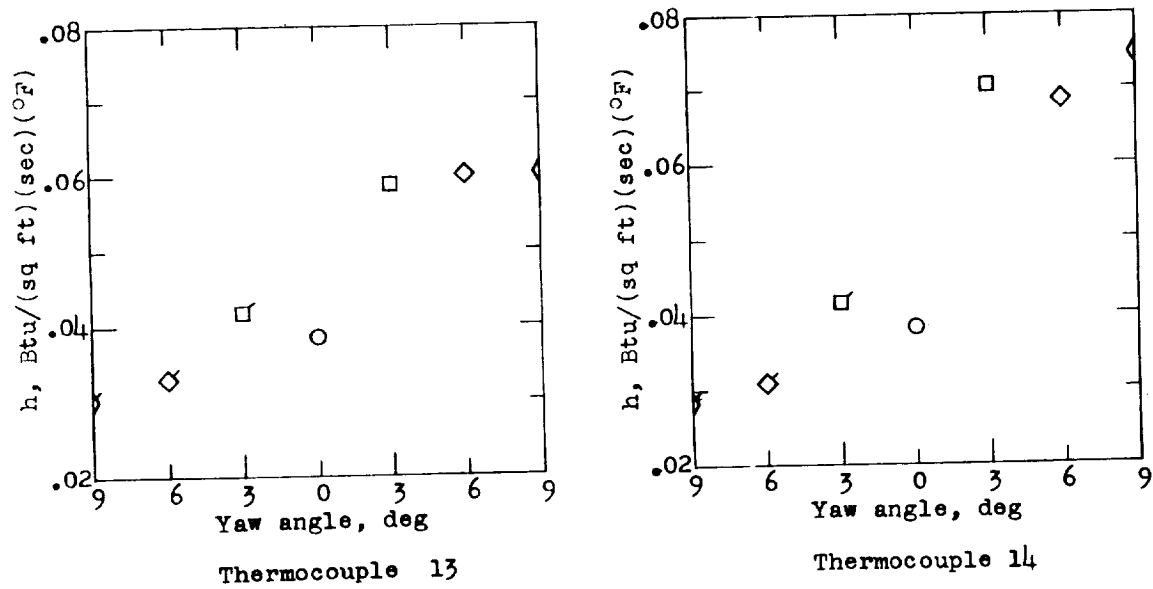


Figure 7.- Concluded.

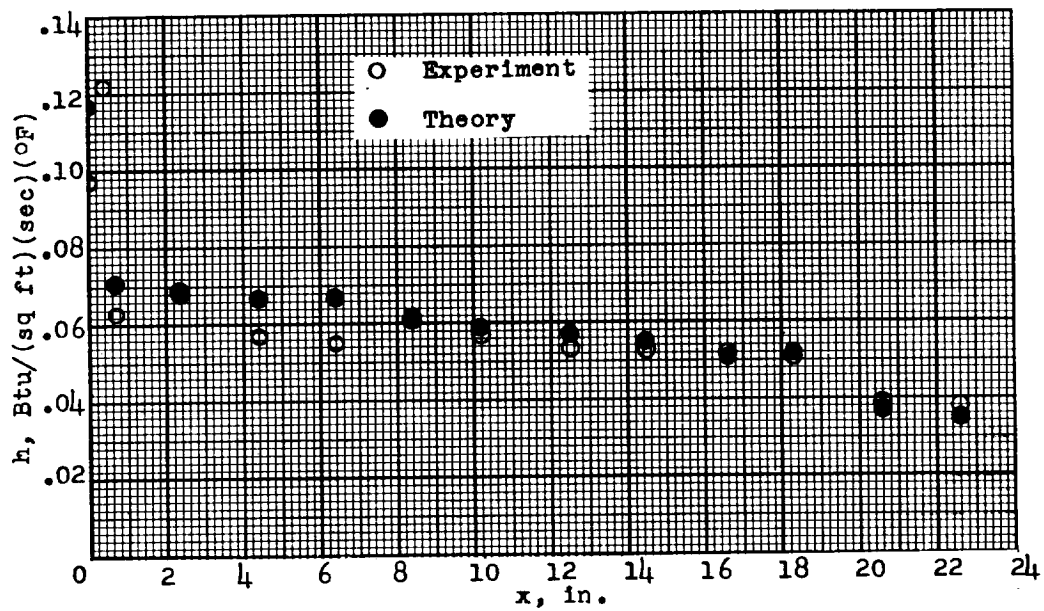
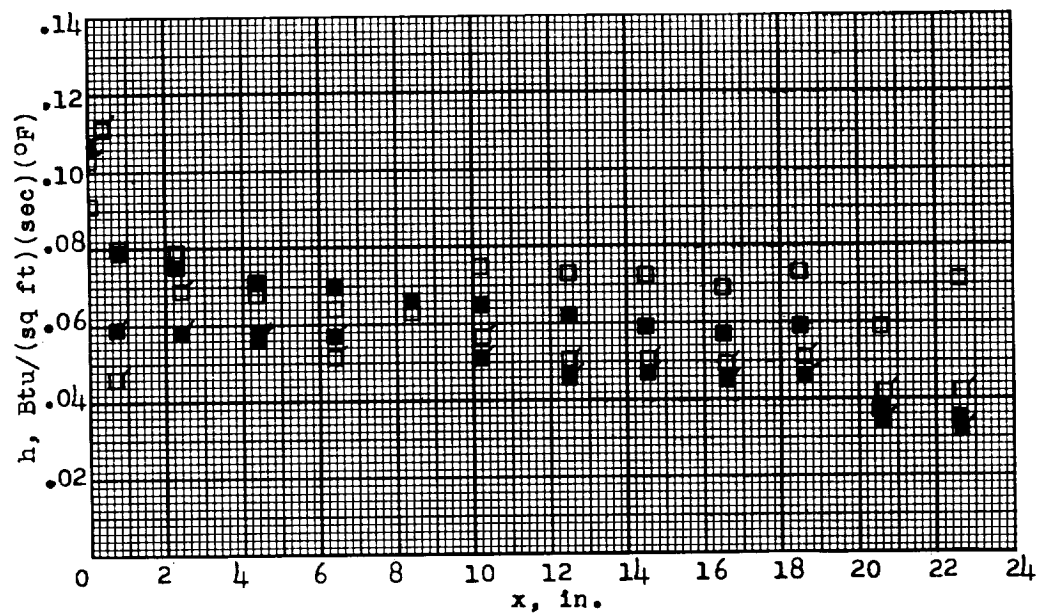
(a)  $\psi = 0^\circ$ .(b)  $\psi = 3^\circ$ .

Figure 8.- Comparison of experimental and theoretical heat-transfer coefficient. Flagged symbols denote leeward side.

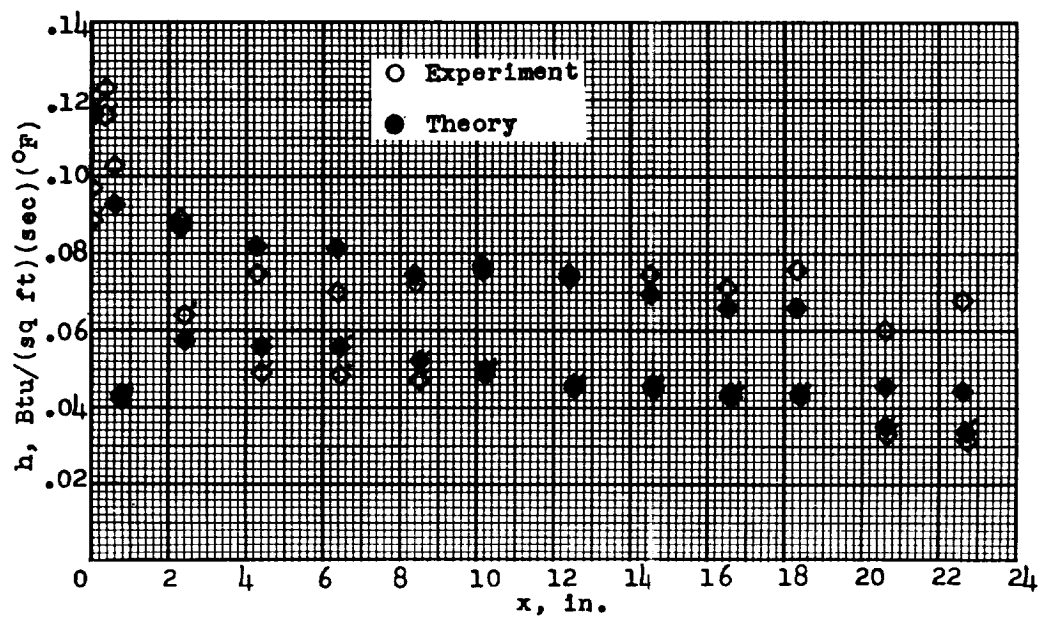
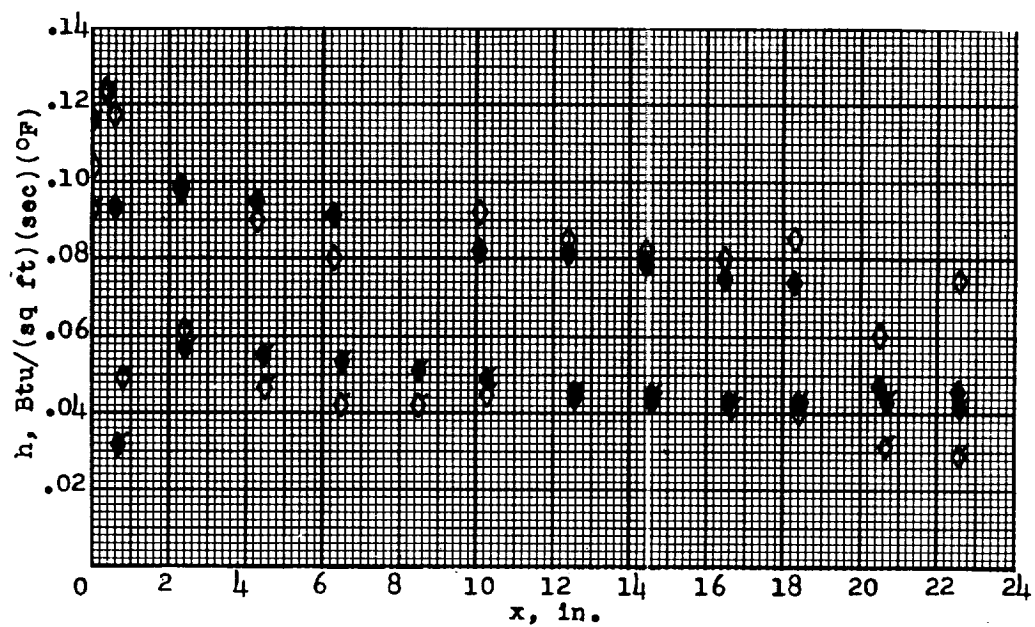
(c)  $\psi = 6^\circ$ .(d)  $\psi = 9^\circ$ .

Figure 8.- Concluded.